

# INTERNATIONAL SOCIETY FOR SOIL MECHANICS AND GEOTECHNICAL ENGINEERING



*This paper was downloaded from the Online Library of the International Society for Soil Mechanics and Geotechnical Engineering (ISSMGE). The library is available here:*

<https://www.issmge.org/publications/online-library>

*This is an open-access database that archives thousands of papers published under the Auspices of the ISSMGE and maintained by the Innovation and Development Committee of ISSMGE.*

*The paper was published in the proceedings of the 20<sup>th</sup> International Conference on Soil Mechanics and Geotechnical Engineering and was edited by Mizanur Rahman and Mark Jaksa. The conference was held from May 1<sup>st</sup> to May 5<sup>th</sup> 2022 in Sydney, Australia.*

# Modelling the effect of in-soil temperature and relative humidity on performance of PET strap soil reinforcement products

Modélisation de l'effet de la température et de l'humidité relative du sol sur les performances des produits de renforcement des sols à base de sangles en PET

**Aníbal Moncada**

*Universitat Politècnica de Catalunya-BarcelonaTech (UPC)*

Ivan P. Damians

*Universitat Politècnica de Catalunya-BarcelonaTech (UPC), International Centre for Numerical Methods in Engineering (CIMNE), and VSL Construction Systems, Spain*

Sebastià Olivella

*Universitat Politècnica de Catalunya-BarcelonaTech (UPC) and International Centre for Numerical Methods in Engineering (CIMNE), Spain*

Richard J. Bathurst

*GeoEngineering Centre at Queen's-RMC, Civil Engineering Department, Royal Military College of Canada, Canada*

**ABSTRACT:** Polyester (PET) strap reinforcement materials are now used routinely as soil reinforcement for mechanically stabilized earth (MSE) walls. The important role of temperature and relative humidity on the chemical degradation of PET fibres due to hydrolysis is well documented in the literature. Strength and stiffness of the polyester fibres can be expected to decrease with increasing temperature and in the presence of moisture. This has practical implications for the selection of the partial factor for chemical degradation that is used in internal stability limit state design in MSE walls. The PET multi-filament core of the straps is protected against installation damage and moisture by a polyethylene sheath. This study presents the results of analyses using numerical simulations that were carried out to estimate, first, the in-soil temperature and relative humidity changes for different ground properties and atmospheric boundary conditions, and second, the temporal strength and stiffness changes in simulated buried PET straps placed in different soil environments while subjected to different tensile loads and temperatures. The soil properties in the analyses are moisture content, hydraulic conductivity (i.e., soil moisture retention curve), soil porosity and intrinsic permeability.

**RÉSUMÉ:** Les matériaux d'armature en sangle de polyester (PET) sont maintenant utilisés couramment comme renforcement du sol pour les murs en terre stabilisée mécaniquement (MSE). Le rôle important de la température et de l'humidité relative sur la dégradation chimique des fibres de PET due à l'hydrolyse est bien documenté dans la littérature. On peut s'attendre à ce que la résistance et la rigidité des fibres de polyester diminuent avec l'augmentation de la température et en présence d'humidité. Ceci a des implications pratiques pour la sélection du facteur partiel pour la dégradation chimique qui est utilisé dans la conception de l'état limite de stabilité interne dans les murs MSE. Le noyau multifilamentaire en PET des sangles est protégé contre les dommages causés par l'installation et l'humidité par une gaine en polyéthylène. Cette étude présente les résultats d'analyses utilisant des simulations numériques qui ont été effectuées pour estimer, premièrement, les changements de température et d'humidité relative dans le sol en fonction des différentes propriétés du sol et des conditions limites atmosphériques, et deuxièmement, les changements temporels de résistance et de rigidité dans des sangles simulées en PET enterrées placées dans différents environnements de sol et soumises à différentes charges de traction et températures. Les propriétés du sol utilisées dans les analyses sont la teneur en eau, la conductivité hydraulique (i.e., la courbe de rétention d'humidité du sol), la porosité du sol et la perméabilité intrinsèque.

**KEYWORDS:** reinforced soil walls, polyester straps, THM modelling, in-soil temperature and relative humidity distribution.

## 1 INTRODUCTION.

Polymeric reinforcement materials are used routinely in civil engineering works for soil reinforcement and stabilization. Geosynthetic materials have proven to be a sustainable solution for mechanically stabilized earth (MSE) wall applications. (Dixon et al. 2017, Damians et al 2018).

In mechanically stabilized earth structures, the crucial role of temperature and relative humidity on the mechanical and chemical degradation of polyester (PET) fibres due to hydrolysis is well documented in the literature (Jailloux et al. 2008, Greenwood et al. 2012). Strength and stiffness of the polyester fibres can be expected to decrease with increasing temperature and in the presence of moisture. These reductions modify the partial factor for creep and chemical degradation that is used in internal stability limit state design for PET strap MSE walls.

Hence, local ambient conditions should be accounted for at the design phase. The PET multi-filament core of the straps is protected by a polyethylene sheath to mitigate installation damage and moisture deterioration. Nevertheless, this sheath still permits the exposure of the polyester filaments to moisture over the life of reinforcement. For instance, high density polyethylene (HDPE) coatings are permeable to water vapor over the long term and thus moisture can accumulate in the air voids between the PET fibres. The rate of degradation due to hydrolysis leading to creep deformation will change with temperature, which can vary widely depending on the environment in which the straps are placed, and temporally with time of day and season. In order to analyze the long-term behaviour of PET straps, the present study proposes a coupled finite element model in which the in-soil distribution of temperature and relative humidity for different atmospheric conditions are evaluated first. Next, visco-

elastic and visco-plastic models are implemented to simulate PET strap long-term response calibrated using the laboratory results of You-Kyum et al. (2018) for GECO's FASTEN FS products (GECO 2021). Finally, a linear coupled thermo-hydro-mechanical MSE wall 2D model is proposed as a preliminary approach.

## 2 ATMOSPHERIC EFFECTS

Previous studies have shown that ambient boundary temperatures can have considerable effect on in-soil temperatures in MSE wall backfills, especially near the surface (Segrestin and Jailloux 1988, Kazosi et al. 2015, Bathurst 1992). Furthermore, backfill temperatures have been shown to follow an annual cyclic pattern (Murray and Farrar 1988). As the depth increases, in-soil temperature tends to a constant value that can be approximated by the annual mean ambient temperature. As such, the average backfill temperature for MSE walls, depending on the geographic location, can be higher than the values presented in design standards (Kazosi et al. 2015).

Thermal models for MSE walls found in the literature (Murray and Farrar 1988, Segrestin and Jailloux 1988, Kazosi et al. 2015) have modelled temperature series data by sinusoidal curves. In this study, daily reported in-situ measurements for various locations were used directly from weather databases (WeatherOnline Ltd) in order to evaluate the effect of different climates (e.g., continental, Mediterranean, desert and tropical) on in-soil temperature and relative humidity propagation with depth.

While some previous studies have shown the importance of soil suction and the impact of precipitation on soil saturation (e.g., Vahedifard et al. 2017), the present preliminary approach does not consider rainfall effects. The influence of rainfall is considered indirectly by the daily ambient temperature and relative humidity data used in this study.

## 3 POLYESTER STRAP REINFORCEMENT BEHAVIOUR

The design process for MSE walls including PET strap walls require the use of partial factors to account for product-specific reduction in mechanical strength due to installation damage, chemical weathering (mainly due to UV light exposure), environmental degradation (primarily due to hydrolysis), and creep (ISO 20432:2007). The determination of partial factors must be based on laboratory testing. In most cases, the degradation caused by UV light can be avoided with proper protection of the material prior to installation. Installation damage must be accounted for by considering the project-specific backfill material and the type of sheath protecting the polyester fibres.

On a short-term basis, the tensile behaviour of PET straps is measured using constant rate of deformation laboratory tests (e.g., ASTM D4595-17, EN ISO 10319:2015). Manufacturers usually offer product lines with a range of tensile resistance (grades), ranging from 30 kN to 100 kN per strap. Like other reinforcement geosynthetics, the strength and stiffness of PET straps is load-, time- and temperature-dependent (Bathurst and Naftchali 2021). Long-term deformation (creep) can be measured under constant tensile load for a given time and constant temperature (ASTM D5262-97). The stepped isothermal method can also be used (ASTM D6992-03).

Creep under constant tensile load can be divided into three stages characterized by (1) a decreasing rate of elongation, followed by (2) a constant rate of strain over time, concluding with (3) an increasing rate of strain over time until rupture. PET strap reinforcement typically exhibits primary and tertiary creep stages (Greenwood et al. 2012). Figure 1 shows constant load creep curves for a FASTEN PET strap product presented as strain versus log time.

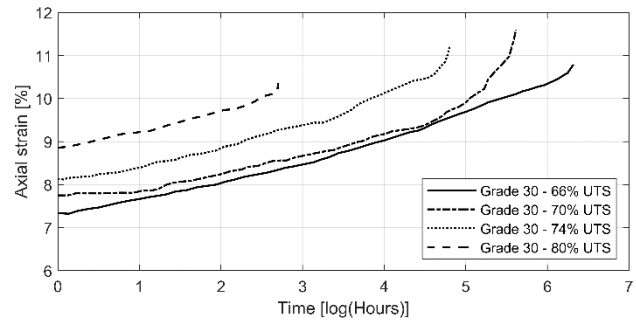


Figure 1. Axial strain versus log time under constant load for grade 30 PET strap reinforcement specimens (You Kyum et al 2018). Note: UTS = ultimate tensile strength.

When water molecules come in contact with polyester, a progressive rupture of the polymer chains results in loss of strength of the material, which is known as degradation by hydrolysis (Jailloux et al. 2008, Greenwood et al. 2012). Laboratory tests to determine the level of degradation due to hydrolysis are carried out by completely submerging samples at high water temperature (98°C), accounting for a fully saturated medium for a period of 28 days (EN 12447-02:2001). As the rate of hydrolysis is sensitive to temperature and relative humidity, the in-soil conditions of MSE walls seem crucial for the determination of a safety factor regarding the expected degradation of the reinforcement caused by hydrolysis. Typical values for chemical degradation partial factors range from 1.0 to 1.4 (ISO 20432:2007).

## 4 NUMERICAL MODEL

The numerical simulations in this study considering environmental effects and PET strap mechanical response were carried out using the software CODE\_BRIGHT (Olivella et al. 1996, CODE\_BRIGHT 2021). This code is used to solve coupled thermal, hydraulic and mechanical problems.

### 4.1 General features

The geometry of the thermal-hydro coupled (TH) model is presented in Figure 2. In order to model the in-soil behaviour due to temperature and relative humidity from the ambient in-air data, a 15 m-high reinforced soil wall was assumed (tall enough to identify in-soil propagation of temperature and relative humidity). The upper boundaries are in direct contact with the atmosphere (i.e., no surface material such as vegetation or pavement is considered). The generated 2D mesh consists of 5536 structural quadrilateral elements with 5714 nodes. Mesh construction included all mechanical elements such as the 1.5 m-high concrete facing panels, the 20 mm-thick bearing pads and the 3 mm-thick PET reinforcement layers with 0.7H length. Mesh sensitivity analyses were first carried out to optimize element size, especially at the boundary surfaces where the ambient in-air boundary conditions are applied. The water table in this study was located at 10 m depth below the ground surface at the wall toe (i.e., at 10 m-height from model bottom). The bottom base temperature was constant at +2°C higher than the mean annual temperature reported from the temperature registry used for each analysis. Staged construction was not used in this study to simplify the model.

Actual real time series input data were used for temperature and relative humidity for each control location, rather than smoothed or simulated sinusoidal temperature ( $T$ ) and relative humidity ( $RH$ ) distributions. Boundary conditions consist of ambient in-air data from daily records including  $T$  (daily minimum and maximum) and  $RH$  that included flux at all surface boundaries in contact with the air (see Figure 2). Points A, B and C, located 2 m from facing and at 1, 7 and 14 m-depth, respectively, were used as measuring points to compare results.

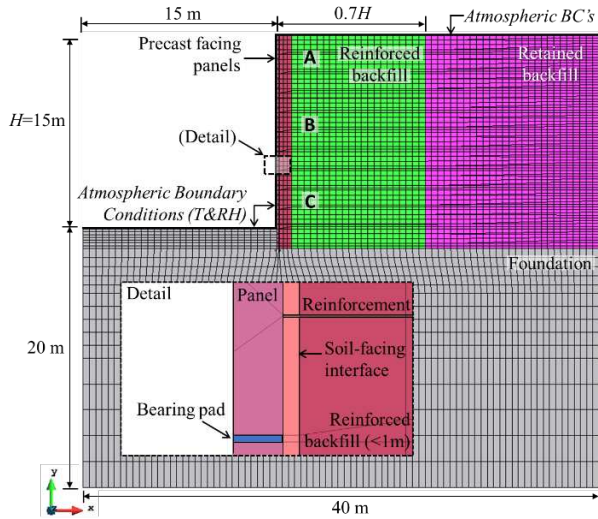


Figure 2. 2D model domain and finite element mesh used for analyses. Note: BC = boundary conditions.

$T$  and  $RH$  environmental data were obtained at four different geographic locations in order to analyze a range of worldwide conditions. The locations corresponded to continental (Toronto), Mediterranean (Barcelona), desert (Abu Dhabi) and tropical (Singapore) climates. Analyses for each model were for 1-, 3- and 5-year periods using daily records from years 2016 through 2020. Figure 3 illustrates a sample of  $T$  and  $RH$  data from the Barcelona 2020 registry, used as boundary conditions for the model for that location.

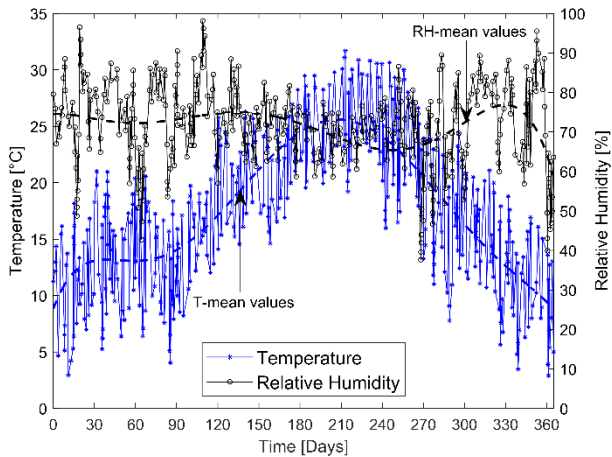


Figure 3. Temperature and relative humidity data from Barcelona 2020 registry (WeatherOnline Ltd).

#### 4.2 Hydraulic and thermal properties

A granular soil was considered in this study. The hydraulic and thermal model formulations and matching soil material parameters are presented in Table 1. Soil thermal dispersion is modeled by Fick's law with a horizontal and vertical dispersivity of  $d_h = 5$  m and  $d_v = 0.5$  m, respectively. Thermal conductivity was modelled using Fourier's law, with dry and saturated conductivity values of  $\gamma_{dry} = 0.5$  W/mK and  $\gamma_{sat} = 1$  W/mK. Default values for solid phase specific heat ( $c_s = 1000$  Jkg<sup>-1</sup>K<sup>-1</sup>) and density ( $\rho_s = 2700$  kgm<sup>-3</sup>) were also used. The water retention curve (Van Genuchten model) for the concrete facing panels was modelled with a reference pressure  $P_0 = 0.001$  MPa and shape parameter  $\lambda = 0.4$ . Table 2 shows porosity and intrinsic permeability values used in the model. Values for the PET strap reinforcement layers, precast facing panels and HDPE bearing

pads correspond have been adjusted to equivalent values for a 2D plane strain 1-m slice.

Table 1. Thermal and hydraulic properties for model soil.

Constitutive law	Formulation	Parameter	Value
Water retention curve (Van Genuchten)	$S_e = \frac{S_l - S_{rl}}{S_{ls} - S_{rl}} = \left(1 + \left(\frac{P_g - P_l}{P}\right)^{\frac{1}{1-\lambda}}\right)^{-\lambda}$	Residual saturation, $S_{rl}$ [-]	0
		Maximum saturation, $S_{ls}$ [-]	1
		Reference pressure, $P_0$ [MPa]	0.005
		Shape parameter, $\lambda$ [-]	0.8
Relative liquid phase permeability	$k_{rl} = S_e^n$	Shape Parameter, $n$ [-]	3

Table 2. Porosity and permeability values for model materials.

Material	Initial porosity [-]	Intrinsic permeability [m <sup>2</sup> ]
Soil (Backfills and Foundation)	0.3	$1 \times 10^{-12}$
Precast facing panels	0.15	$1 \times 10^{-12}$
PET strap reinforcements	0.01	$1 \times 10^{-16}$
HDPE bearing pads	0.4	$1 \times 10^{-10}$

#### 4.3 PET straps mechanical properties

Short-term behaviour of PET straps can be modelled using linear stress-strain relationships. The present study considers two cases, a linear model with a single elastic modulus, and a bi-linear model with two elastic moduli.

In order to simulate in-soil conditions acting over the PET strap reinforcement, a temperature- and saturation-dependent visco-elastic (VE) constitutive model was used to account for creep, with rate of deformation ( $d\varepsilon/dt$ ) and viscosity ( $\eta$ ) formulated as (Eq.1) and (Eq.2), respectively:

$$\frac{d\varepsilon}{dt} = \frac{1}{2\eta^{VE}} (\sigma' - p'I) \quad (1)$$

$$\frac{1}{\eta^{VE}} = B(T)\sqrt{S_l} \quad (2)$$

Here,  $\sigma'$  is effective stress,  $p'$  is mean stress,  $I$  is the identity matrix,  $S_l$  is degree of saturation and  $B(T)$  is a function of temperature ( $T$ ), the universal gas constant ( $R$ ), and activation energy ( $Q$ ).

Additionally, a visco-plasticity (VP) model was implemented to account for strain softening over long-term constant load. (Eq.3-5):

$$\frac{d\varepsilon^{VP}}{dt} = \Gamma \langle \Phi(F) \rangle \frac{\partial G}{\partial \sigma} \quad (3)$$

$$\Phi(F) = F^m \quad (4)$$

$$\Gamma = \Gamma_0 \exp\left(\frac{-Q}{RT}\right) \quad (5)$$

Here,  $F$  and  $G$  are functions of mean stress ( $p$ ), a frictional parameter ( $\delta$ ) and adhesion ( $a$ ), and  $m$  is a power stress parameter. Parameter  $\Gamma$  is fluidity which is a function of temperature, reference fluidity ( $\Gamma_0$ ), universal gas constant ( $R$ ), and activation energy  $Q$ . Parameters  $\delta$  and  $a$  are controlled by a softening parameter ( $\eta^*$ ) which provides a transition between peak and residual stages.

The mechanical parameters used to model the PET straps are presented in Table 3. Since the implemented model is 2D (i.e., 1 m-plane strain slice), an equivalent plane strain stiffness was calculating considering an average width of 89 mm per strap and two connections every 2.5 m in the wall face direction (i.e., single panel width) (see Damians et al. 2021). A linear model with an elastic modulus  $E = 32$  GPa and Poisson's ratio  $\nu = 0.2$  was used to model the precast concrete facing panels.

Table 3. Model parameters for PET strap reinforcement

Constitutive model	Parameter	Value
Linear elasticity	Elastic modulus, $E$ [MPa]	2.2 to 4.8
	Poisson's ratio, $\nu$ [-]	0.30 to 0.34
Bi-linear elasticity	1 <sup>st</sup> elastic modulus, $E_1$ [MPa]	1.7 to 3.9
	2 <sup>nd</sup> elastic modulus, $E_2$ [MPa]	45 to 100
	Poisson ratio, $\nu$ [-]	0.20 to 0.33
Visco-elasticity (VE)	Volumetric strain limit for $E_i$ change, $\epsilon_{v\text{-limit}}$ [-]	0.0078 to 0.086
	Fluidity, $B$ [ $s^{-1}MPa^{-1}$ ]	$5.3 \times 10^{-14}$ to $2.1 \times 10^{-10}$
Visco-plasticity (VP)	Power of stress function, $m$ [-]	2.6 to 3.8
	Fluidity, $\Gamma$ [ $s^{-1}MPa^{-m}$ ]	$3.6 \times 10^{-4}$ to $1.4 \times 10^{-3}$
	Softening parameter, $\eta^*$ , [-]	$1 \times 10^{-3}$ to $8 \times 10^{-2}$
Visco-plasticity (VP)	Peak & residual parameters for adhesion, $a_{\text{peak}}$ & $a_{\text{res}}$ [MPa]	0.05 to 0.12 and 0.03 to 0.12
	Peak & residual parameters for friction, $\delta_{\text{peak}}$ & $\delta_{\text{residual}}$ [°]	$10^{-4}$ and $10^{-5}$

Two scenarios were analyzed. First, elements with bi-linear elastic moduli and VE properties were subjected to an initial tension, followed by a ramp increase up to the desired load representing a selected fraction of the ultimate tensile strength (UTS). Second, elements with linear elastic modulus, VE and VP properties were subjected to a constant initial load.

## 5 RESULTS

### 5.1 Atmospheric effect modelling

Figure 4 and Figure 5 show  $T$  and  $RH$  distribution over a 1-year analysis period for Barcelona 2020 in-air (atmospheric) conditions. Model results show an important variation of temperature ( $\Delta T \approx 8^\circ\text{C}$ ) within the first 2 meters from the domain air boundaries, followed by a 4-meter zone in which variations are visible but less pronounced ( $\Delta T \approx 2^\circ\text{C}$ ). As depth increases, in-soil  $T$  appears to remain unaffected and converges to the imposed lower boundary condition.

Regarding  $RH$ , a zone of influence of 1 m can be identified at the air boundaries. At depth, an increasing gradient can be observed, reaching saturation near the imposed water table. Depending on the observation period, the backfill as a whole, shifts from a saturated air condition to  $RH$  values as low as 50%. Due to the open joints between panels (2 bearing pads per panel) propagation zones due to diffusive flow through these openings can be seen.

Figure 6 shows the variation of  $T$  and  $RH$  at points A, B and C (locations shown in Figure 2), for Abu Dhabi, Barcelona, Toronto, and Singapore ambient air conditions. As depth increases, the variations in  $T$  go from  $10^\circ\text{C}$  at 1 meter to a stable  $4^\circ\text{C}$  variation at 14 and 21 meters for all conditions with the exception of Singapore, which remains at a steady  $29^\circ\text{C}$  at all observation points. It can be noted that the effect of ambient temperature delays changes for in-soil  $T$ . As depth increases the peaks of temperature distribution curves are present at a later time with respect to surface values. The same latency can be observed in  $RH$  variations. Mean model temperatures were  $29^\circ\text{C}$ ,  $17^\circ\text{C}$ ,  $28^\circ\text{C}$ , and  $10^\circ\text{C}$  for Abu Dhabi, Barcelona, Singapore, and Toronto, respectively. Different environmental conditions result in wide in-soil variation of  $RH$ , ranging from 45-100% and 13-100% for Barcelona and Abu Dhabi and 62-100% and 31-100% for Singapore and Toronto, respectively. As discussed earlier, laboratory hydrolysis testing was carried out at a constant  $RH = 100\%$ . The numerical results at lower  $RH$  values suggests that a slower rate of chemical degradation of PET strap reinforcement would occur for the simulated conditions in this study. Nevertheless, results show air saturation ( $RH = 100\%$ ) occurs for periods of 100 days or more during the one-year cycle for

Barcelona and Toronto.  $RH$  tends to higher values as depth increases. Increases of  $RH$  within the soil due to lower temperatures can be observed. It must be noted that the current model does not account for surface precipitation which could potentially change the in-soil  $T$  and  $RH$  distributions. Mean  $RH$  values for Abu Dhabi, Barcelona, Singapore and Toronto atmospheric conditions were 59%, 86%, 85% and 84%, respectively for the same A-B-C observation points over a 1-year analysis.

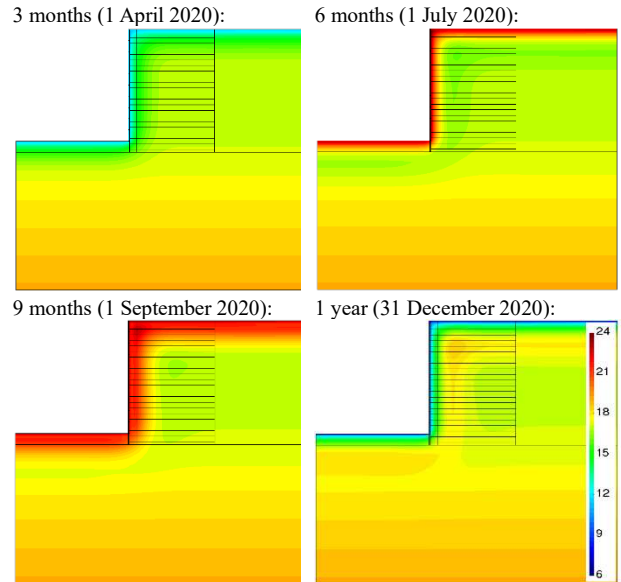


Figure 4. TH model 1-year temperature ( $^\circ\text{C}$ ) results for Barcelona 2020.

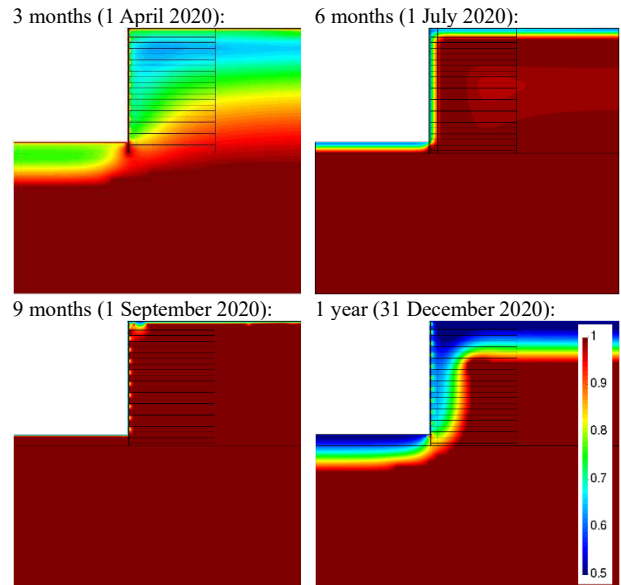


Figure 5. TH model 1-year relative humidity (-) results for Barcelona 2020.

Figure 7 shows the temperature variation of a vertical soil profile at 4 meters from the wall facing over a 5-year period using the Barcelona registry. Results show that  $T$  changes within the first 3 meters constitute the largest fluctuations matching the prescribed boundary conditions ( $3^\circ\text{C}$  to  $30^\circ\text{C}$ ). From 3 to 15 meter-depth,  $T$  fluctuations diminish and begin oscillating within  $\pm 2^\circ\text{C}$  with respect to the annual mean atmospheric temperature ( $17^\circ\text{C}$ ). Below 15 meters,  $T$  stabilizes with less than  $\pm 1^\circ\text{C}$  variation and approaches a constant value matching the lower boundary condition.

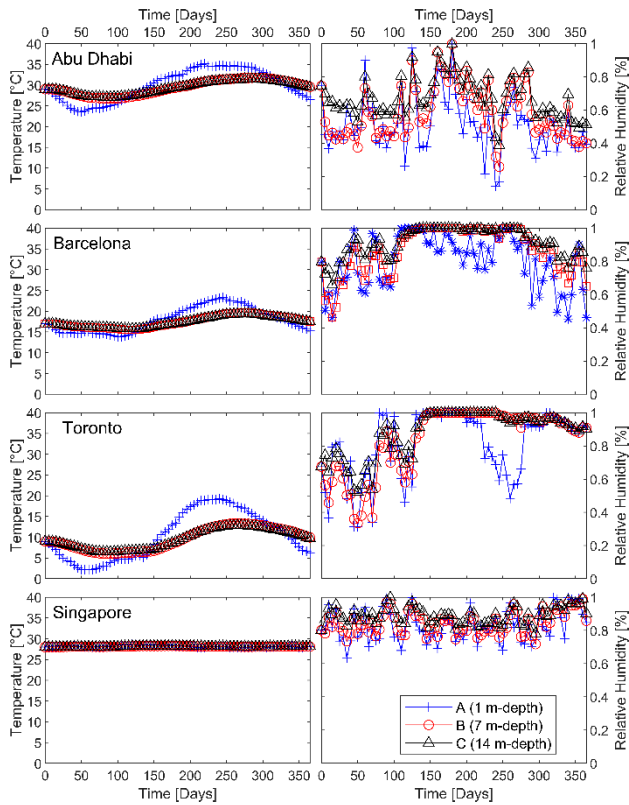


Figure 6. Evolution of temperature and relative humidity at points A, B and C for the four different locations and climates considered.

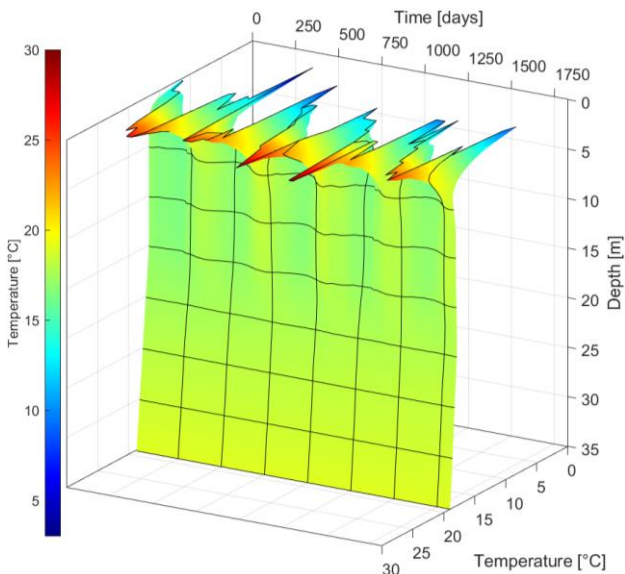


Figure 7. In-soil temperature distribution over a 5-year period using Barcelona climate data and sand backfill model.

### 5.2 PET strap modelling

Figure 8 depicts the adjustment of the proposed models with creep laboratory measurements obtained by You-Kyum et al. (2018) for grade 30, 50 and 70 kN straps under loads of 66% and 70% of UTS. The obtained adjustment is adequate for both the bi-linear elastic and VE models, and VE and VP models. Figure 9 illustrates the influence of temperature on creep behaviour for a grade 30 reinforcement material under 70% UTS load at constant temperature. The range of temperatures used (10°C and 29°C) are the maximum and minimum mean values obtained using the thermo-hydraulic models with different ambient in-air conditions. When subjected to temperature variations, both the

VE and VP models update their equivalent fluidity, thus, long-term deformation varies within a range of 1-1.5% for a 19°C variation over a 50-year period. By including a linear expansive model, an initial change in temperature (from 20°C to 10°C or 20°C to 29°C), followed by a constant temperature modelling, shifts the creep curve to higher or lower deformation for increasing or decreasing temperatures, respectively.

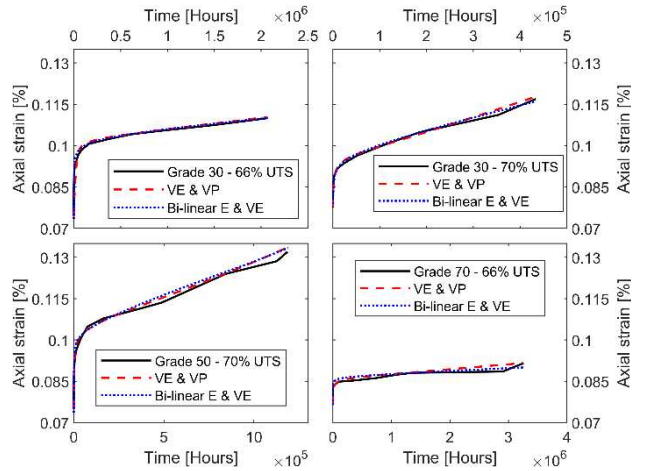


Figure 8. Long-term deformation model results for grades 30, 50 and 70 kN at 66 or 70% of UTS load compared to accelerated laboratory creep tests.

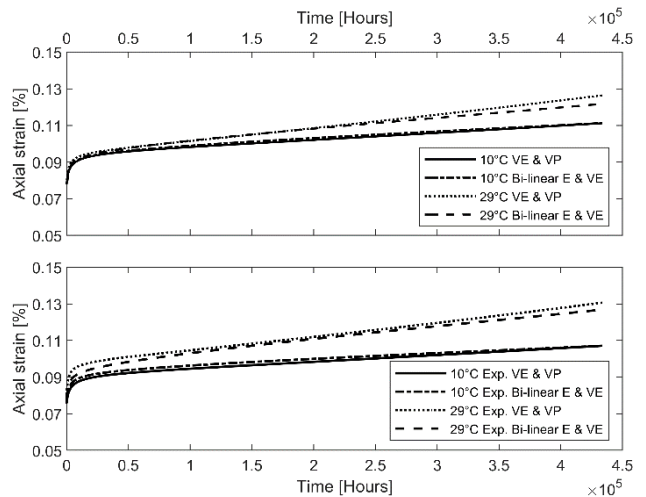


Figure 9. Creep behavior changes due to temperature variations from 20°C to 10°C or 29°C for a grade 30 strap at 70% UTS load.

As a first approach, a linear elastic reinforcement model with creep (bi-linear elasticity and VE model) was used together with linear elastic concrete and backfill materials for the thermo-hydro-mechanical (THM) model case geometry in Figure 2.

Figure 10 presents horizontal displacements of the deformed mesh for a 1-year analysis period using Barcelona atmospheric boundary conditions with the bi-linear elastic and VE PET strap model. Since the analysis is limited to one year, no significant variations were observed between different boundary condition cases. When comparing linear elastic and VE model results, the maximum displacement increases by about 4% over a 1-year period for the VE model.

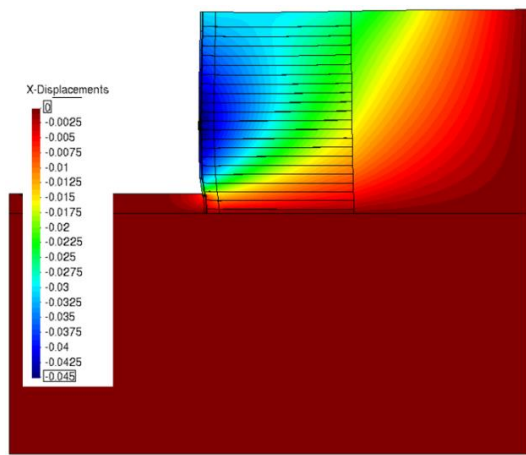


Figure 10. Horizontal outward displacements (m) and deformed mesh (amplification factor  $\times 10$ ) after 1 year analysis with an elastic coupled THM model with PET straps reinforcements (bi-linear elastic and VE model) using Barcelona 2020 atmospheric registry.

## 6 CONCLUSIONS

The present study demonstrates the implementation of a hydro-thermal model to evaluate the effects of prolonged ambient conditions on in-soil conditions with different ambient environmental conditions on the backfill soil, and the long-term behaviour of the embedded PET strap reinforcement layers used in MSE walls. Linear elastic models for the MSE wall components were used together with a coupled THM model for the soil as an initial approach.

TH models gave results in accordance with previous studies (e.g., Segrestin and Jailloux 1988, Kazosi et al. 2015) for temperature distributions in-soil as a function of depth. The mean in-soil temperature ( $T$ ) can be approximated by the annual mean environmental (atmospheric) in-air values. Over the first 1 to 3 meters, fluctuations of approximately  $\pm 10^\circ\text{C}$  were observed, depending on the applied boundary environmental conditions. From 3 to 15 meters,  $T$  variations are reduced to  $\pm 2^\circ\text{C}$ . At depths greater than 15 meters,  $T$  remains constant, converging to the lower boundary-imposed value. Mean annual temperatures used as boundary conditions ranged from  $10^\circ\text{C}$  to  $29^\circ\text{C}$ . Regarding  $RH$ , air saturation was achieved after 100 days for Barcelona and Toronto climate registry cases, with a mean value of 86% and 84%, respectively. For desert ambient conditions (Abu Dhabi), air saturation was rarely observed, with a mean  $RH$  of 59% at the observation depths. The tropical environment case (Singapore) resulted in almost constant  $RH$  values of 85% throughout the analysis period. The effect of PET strap hydrolysis was measured using fully saturated laboratory specimens. These data are useful to estimate the long-term degradation of the PET straps when in-soil  $RH$  humidity periodically reaches full saturation.

Visco-elastic and visco-plastic models were fitted to creep master curves with satisfactory results for different grades of PET straps and a range of UTS loads. The proposed models incorporate temperature dependencies and, as such can prove useful when modelling the effect of in-soil conditions on long-term deformations for these soil reinforcement materials.

## 7 ACKNOWLEDGEMENTS

The authors wish to thank Aaron Kim from GECO Industrial (Korea, Rep.) for providing data for polymeric straps (FASTEN products) from reliability assessment testing records.

## 8 REFERENCES

ASTM D4595-17. 2017. Standard Test Method for Tensile Properties of

- Geotextiles by the Wide-Width Strap Method, ASTM International, West Conshohocken, PA, USA.
- ASTM D5262-97. 1997. Standard Test Method for Evaluating the Unconfined Tension Creep Behavior of Geosynthetics. ASTM International, West Conshohocken, PA, USA.
- ASTM D6992-03. 2003. Standard Test Method for Accelerated Tensile Creep and Creep-Rupture of Geosynthetic Materials Based on Time-Temperature Superposition Using the Stepped Isothermal Method. ASTM International, West Conshohocken, PA, USA.
- Bathurst, R.J. 1992. Case study of a monitored propped panel wall. In Proceedings of the International Symposium on Geosynthetic-Reinforced Soil Retaining Walls, Denver Colorado, pp. 159-166, August 1991 (published by A.A. Balkema).
- Bathurst, R.J., and Naftchali, F.M. 2021. Geosynthetic reinforcement stiffness for analytical and numerical modelling of reinforced soil structures. *Geotextiles and Geomembranes*, 49, 921-940.
- CODE BRIGHT User's Guide. 2021. Department of Civil and Environmental Engineering, Universitat Politècnica de Catalunya-BarcelonaTech (UPC) and International Center for Numerical Methods in Engineering (CIMNE). [https://deca.upc.edu/en/projects/code\\_bright](https://deca.upc.edu/en/projects/code_bright)
- Damians, I.P., Bathurst, R.J., Adroguer, E.G., Josa, A. and Lloret, A. 2018. Sustainability assessment of earth retaining wall structures. *Environmental Geotechnics* 5 (4), 187-203.
- Dixon, N., Fowmes, G., and Frost, M. 2017. Global challenges, geosynthetic solutions and counting carbon. *Geosynthetics International*, 24(5), 451-464.
- EN 12447-02. 2001 Geotextiles and geotextile-related products – Screening test method for determining the resistance to hydrolysis in water. CEN/TC 189, European Standard.
- GECO 2021. GECO Industrial Co., Ltd. Gyeonggi-do, Republic of Korea. <http://gecoind.com/en/product/fasten.php>
- Gelhar, L.W., Welty, C., and Rehfeldt, K.R. 1992. A critical review of data on field-scale dispersion in aquifers. *Water Resources Research*, 28(7), 1955-1974.
- Greenwood, J.H., Schroeder, H.F., and Voskamp, W.; 2012. Durability of Geosynthetics (Publication 243). CUR Committee C 187. Building and Infrastructure. ISBN 978-90-376-0533-4.
- ISO 10319-15. 2015. Geosynthetics - Wide-width tensile test. ISO, Geneva, Switzerland.
- ISO/TR 20432:2007. Guidelines for the determination of the long-term strength of geosynthetics for soil reinforcement. ISO, Geneva, Switzerland.
- Jailloux, J.M., Nait-Ali, K.L., and Freitag, N. 2008. Exhaustive long-term study on hydrolysis of high-tenacity polyester-10-year results. In Proceedings of the 4th European Geosynthetics Conference, Edinburgh, UK, 6p.(CD-ROM-Paper 212).
- Kasozi, A.M., Siddharthan, R.V., and Mahamud, R. 2015. Temperature distribution in mechanically stabilized earth wall soil backfills for design under elevated temperature conditions. *Journal of Thermal Science and Engineering Applications*, 7(2).
- Murray, R.T., and Farrar, D.M. 1988. Temperature distributions in reinforced soil retaining walls. *Geotex and Geomem* 7(1-2), 33-50.
- Naughton, P.J., and Kempton, G.T. 2006. Life-time assessment of polyester based geosynthetics. In Proceedings of the 8th International Conference on Geosynthetics, Yokohama, Japan.
- Olivella S, Gens A, Carrera J, Alonso E. 1996 Numerical formulation for a simulator (CODE\_BRIGHT) for the coupled analysis of saline media. *Engineering Computations* 13(7), 87-112.
- Segrestin, P., and Jailloux, J.M. 1988. Temperature in soils and its effect on the ageing of synthetic materials. *Geotex and Geomem*, 7, 51-69.
- Vahedifard, F., Tehrani, F.S., Galavi, V., Ragno, E., and AghaKouchak, A. 2017. Resilience of MSE walls with marginal backfill under a changing climate: Quantitative assessment for extreme precipitation events. *J of Geotech and Geoenviron Engineering*, 143(9), 04017056.
- You-Kyum, K., Gyeong-Yun, S. 2018. Reliability assessment of polymeric straps (FASTEN FS) for soil reinforcement. H411-18-00067. GECO Industrial Co., Ltd. FITI Testing and Research Institute, Chungbuk, Korea.
- WeatherOnline Ltd. Meteorological Services, viewed on March 2021, <https://www.weatheronline.co.uk/>